coatings

MDPI

Article

Study on the Duration of Laser-Induced Thin Film Plasma Flash

Guixia Wang, Junhong Su * and Qingsong Wang

Department of Photoelectric Engineering, Xi'an Technological University, 2 Xue Fu Zhong Lu, Weiyang District, Xi'an 710021, China; noragirl6@126.com (G.W.); wqsxatu@xatu.edu.cn (Q.W.)
* Correspondence: sujunhong@xatu.edu.cn

Abstract: The accuracy of judging whether the film is damaged directly affects the accuracy of the measurement of the film laser damage threshold. When judging the film damage by the traditional plasma flash method, there is a problem of misjudgment caused by the failure to distinguish the film and air plasma flash. In order to eliminate misjudgment, the two flashes are accurately distinguished by the difference in the duration of the air and film plasma flash. This paper aims to obtain the theoretical and experimental values of the duration of the film plasma flash (t_f) and analyze the factors affecting it. Firstly, taking single-layer hafnium oxide and aluminum oxide thin films as examples, when the wavelength of the incident laser is 1064 nm, the diameter of the laser focusing spot is 0.08 cm, the energy of the incident laser is 100 mJ, and the pulse width of incident laser is 10 ns, the t_f of hafnium oxide, and aluminum oxide thin films are 542.7 and 299.6 ns, respectively. Secondly, the experimental study of t_f was carried out. Through six experiments, the following results were obtained: (1) With the increase in incident laser energy, the t_f of both films increases; (2) The t_f of the hafnium oxide film is longer than that of the aluminum oxide film. (3) The experimental parameters are put into the calculation model, and the theoretical results are in good agreement with the experimental t_f values. Finally, it is found that t_f increases with the increase in incident laser energy and incident laser pulse width, and decreases with the increase in focusing spot diameter.

Keywords: laser damage; thin film plasma flash duration; damage identification; damage misjudgment

check for updates

Citation: Wang, G.; Su, J.; Wang, Q. Study on the Duration of Laser-Induced Thin Film Plasma Flash. *Coatings* **2023**, *13*, 1323. https://doi.org/10.3390/coatings13081323

Academic Editor: Olga Krysina

Received: 24 June 2023
Revised: 23 July 2023
Accepted: 25 July 2023
Published: 27 July 2023

1. Introduction

With the application of laser weapons such as laser fusion, laser radar guidance, laser blinding and strong laser destruction, and the development of the "divine light" system, the development trend of laser is gradually towards the direction of high power and high energy [1,2]. The thin film element with a high threshold is one of the necessary devices in the high-power laser system, it is very important in the system, and it is also the most vulnerable link because of its working environment. This requires the thin film element to have good resistance to laser damage. The resistance to laser damage of the thin film element is often evaluated by its laser-induced damage threshold (LIDT). The larger the LIDT of the thin film, the better its resistance to laser damage [3–7]. Therefore, how to obtain high LIDT becomes the main bottleneck to improving the resistance to laser damage of thin film components. One of the keys to solving this problem is the accurate measurement of LIDT of thin films.

The International Committee for Standardization issued the test standard ISO21254. When measuring the LIDT of the film with this standard, it is necessary to test under different ten kinds of laser energy. Each laser energy needs to test ten different positions, and some positions are damaged while the rest are not damaged. In this way, a damage probability can be obtained under each laser energy, and finally, ten damage probabilities can be obtained, and the LIDT of the thin film can be obtained by fitting ten damage probabilities under the action of ten laser energies [8]. Obviously, to ensure the accuracy of measuring the LIDT of thin film, the key is to accurately judge whether the damage occurs at each test point. When the traditional plasma flash method is used for damage

discrimination, sometimes it cannot distinguish the air plasma flash from the thin film plasma flash, which will cause misjudgment and lead to a large error in the measurement of LIDT. When the measured component is applied to the high-energy laser system, it may be damaged in advance, resulting in the failure of the whole system to work normally.

The traditional plasma flash method cannot distinguish the air plasma flash from the thin film plasma flash in damage identification, which leads to misjudgment. In order to improve the accuracy of film damage identification, misjudgment must be eliminated. In fact, in 2011, Lang et al. experimentally found that the duration of the aluminum target plasma flash was about 280 ns, while the duration of the accompanying air plasma flash on the target surface was greater than 7580 ns [9]. Therefore, it is feasible to distinguish the film plasma flash from the air plasma flash by the different duration of the two flashes (t_f and t_c).

In the study of high energy laser induced breakdown of solid to produce plasma, Xia et al. [10] experimentally studied the conditions under which the thermodynamic parameters of thin-film plasma flash changed with time; Yizhong et al. [11] and Ran et al. [12] reported the temporal and spatial evolution of aluminum plasma flash; Tristan et al. [13], Lancry et al. [14], Kim et al. [15], Axente et al. [16], Lian-Bo et al. [17], and Ran et al. [18] obtained many important laws and conclusions related to high energy laser induced breakdown of solids by using high energy laser induced breakdown plasma flash spectra; Nagli et al. [19], Behera et al. [20], and Lan et al. [21] conducted a detailed analysis of the dynamic behavior of aluminum plasmas. In this paper, the authors performed many studies on laser-induced thin film and air plasma flash, and found that the ignition time of the thin film and air plasma flash is on the order of nanosecond, and the air plasma flash is ignited before the thin film plasma flash. Around the plasma flash generated by high energy laser-induced breakdown of solids, the above literature studies the breakdown threshold, the ignition time of plasma flash, the temporal and spatial evolution of plasma flash, and the application of flash spectrum, etc. However, the problem of how to calculate and test the duration of film plasma flash (t_f) has not been solved.

This paper mainly focuses on the theoretical and experimental research of t_f, and analyzes the factors affecting the length of t_f. The specific contents are as follows: (1) build a model and calculate t_f; (2) the experimental value of t_f is obtained, and the experimental and theoretical values of t_f are compared and analyzed. (3) Through the analysis of the established model, the relevant factors affecting the length of t_f were analyzed, and the influence law was found.

2. Theoretical Calculation Model of the Duration of Film Plasma Flash

Generally speaking, the incident laser energy of the air-generated plasma is higher than that of the film-generated plasma, but after the film surface is first broken down, the ejector material generated reduces the breakdown threshold of the air near the film surface, so the film plasma flash will also be accompanied by the air plasma flash. According to the aerodynamic theory, the relation between the pressure p_s of a plasma shock wave in the air and the velocity v_s of the shock wave is [22]:

$$\frac{p_s}{p_0} = [1 + \frac{(\gamma - 1)v_s}{2c_s}]^{\frac{2\gamma}{\gamma - 1}} \tag{1}$$

In the above equation, p_0 is the pressure of air, and $p_0 = 1.01 \times 10^5$ N/m^2; c_s is the speed of sound in air, and $c_s = 340$ m/s; γ is the specific heat ratio of air plasma, and $\gamma = 1.4$. Equation (1) can be obtained after simplification and deformation:

$$v_s = \frac{(\frac{p_s}{p_0})^{1/7} - 1}{0.000588824} \tag{2}$$

According to the literature [23], the pressure of plasma shock wave in the air (p_s) changes with time (t) as follows:

$$p_s = \begin{cases} p_0, t = 0 \\ \rho_0 \frac{{v_L}^2}{\gamma_b+1} \left(\frac{\gamma_b+1}{2\gamma_b} \right)^{\frac{2\gamma_b}{\gamma_b-1}}, 0 < t < t_p \\ \rho_0 \frac{{v_L}^2}{\gamma_b+1} \left(\frac{\gamma_b+1}{2\gamma_b} \right)^{\frac{2\gamma_b}{\gamma_b-1}} \left(\frac{t_p}{t} \right)^{\frac{2}{3}}, t_p \le t \le t_{2D} \\ p_{s20} \left(\frac{t_{2D}}{t} \right)^{\frac{6}{5}}, t_{2D} \le t < t_0 \\ p_0, t \ge t_0 \end{cases} \quad (3)$$

In Equation (3), p_0 is the pressure of air; v_L represents the propagation velocity of detonation wave supported by the laser, $v_L = 0.958 {\rho_0}^{-\frac{1}{3}} P^{\frac{1}{3}}$, where ρ_0 is the air density, $\rho_0 = 1.295$ kg/m^3, and P is the actual incident laser power. If P_0 is used to represent the initial power of incident laser, when the incident laser energy is E, then:

$$P_0 = \frac{4E}{\pi {D_s}^2 t_p} \quad (4)$$

In Formula (4), D_s is the diameter of the focusing spot, P_1 is the radiation loss in the plasma region, and P_2 is the radiation loss caused by inverse bremsstrahlung absorption, then the actual incident laser power density P satisfies the formula $P = P_0 - P_1 - P_2$. If the radiation loss in the plasma region is ignored, then $P = P_0 - P_2$. In the process of laser irradiation, plasma has an inverse bremsstrahlung absorption effect on laser, and the inverse bremsstrahlung absorption coefficient is expressed as [22]:

$$K_s = \frac{2.432 \times 10^{-37}}{(h\upsilon)^3} [1 - \exp(-\frac{h\upsilon}{kT})] {N_e}^2 T^{-1/2} Z^2 \quad (5)$$

In Equation (5), υ is the laser optical frequency and h is Planck's constant. When the incident laser wavelength is 1064 nm, $h\upsilon = 1.1$ ev, k is Boltzmann constant, N_e is the electron number density of the material on the surface of the film, T is the plasma temperature, and Z is the atomic number.

If l is assumed to be the linearity of the plasma, then [22]:

$$P = P_0 - P_2 = \frac{P_0}{\exp^{lk_s}} \quad (6)$$

In Equation (3), γ_b is the adiabatic index of the plasma, which takes a value of 1.2 in the plasma region. The laser pulse width is t_p, and t_{2D} is the time required for to laser supports detonation wavefront extending to the diameter distance of the focusing spot (D_s), then, $t_{2D} = D_s / v_L$. t_0 is the total action time of an air plasma shock wave.

Coupling (2)–(6), set the wavelength of the incident laser $\lambda = 1064$ nm, the diameter of the laser focusing spot $D_s = 0.08$ cm, and the pulse width of incident laser $t_p = 10^{-8}$ s. Take l of HfO_2 and Al_2O_3 film are 0.1 cm and 0.18 cm, respectively, and take the two films $T = 10^5$ K, $N_e = 10^{19}$/cm^3, and $E = 100$ mJ, then the variation curve of plasma shock wave velocity v_s with time t of single layer HfO_2 and Al_2O_3 film can be obtained, respectively, as shown in Figures 1 and 2.

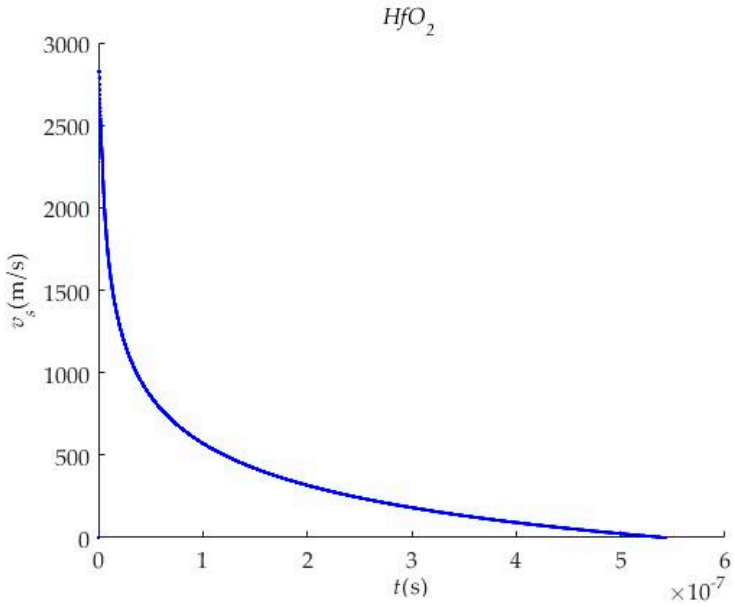

Figure 1. Curve of v_s versus t of the single HfO_2 film.

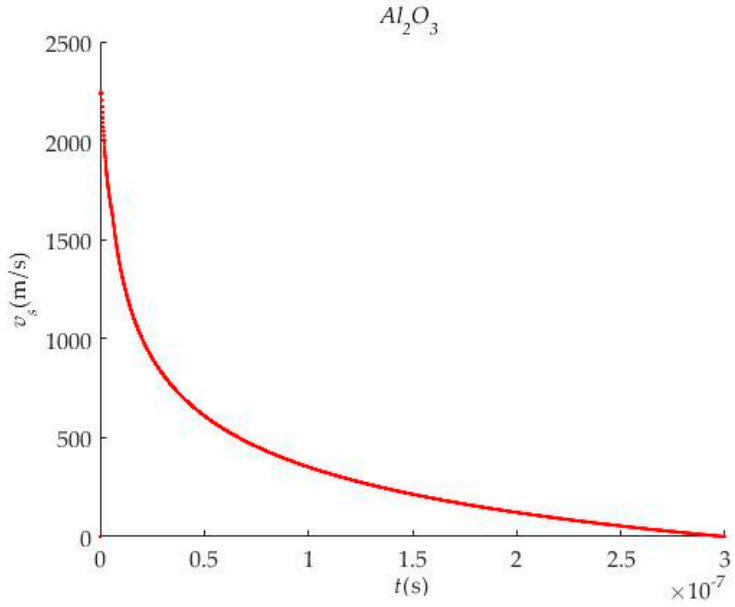

Figure 2. Curve of v_s versus t of the single Al_2O_3 film.

When the film plasma shock wave velocity v_s decreases to zero, the film plasma flash disappears, so it is defined that the film plasma flash duration t_f is equal to the time interval when v_s decreases from the maximum velocity to zero. According to Figures 1 and 2, t_f of single layer HfO_2 and Al_2O_3 film is 542.7 ns and 299.6 ns respectively. This is consistent with the experimental results in the literature [9] that the target surface plasma duration of the target is greater than 280 ns. In addition, it is consistent with the experimental results obtained in the literature [22] that the film plasma shock wave action time is greater than 200 ns.

3. Experimental Study on the Duration of Film Plasma Flash

3.1. Experimental Principle

The experimental schematic diagram is shown in Figure 3. The light source is a high-power Nd:YAG solid state laser, the laser wavelength is 1064 nm, the output energy

is adjustable from 5 mJ to 235 mJ, the focusing spot diameter is 0.08 cm, and the pulse width is 10 ns. After the intense laser emitted by Nd:YAG laser 1 passes through the filter plate 2 and attenuator 3, it is focused by the focusing system 4 and passes through the beam splitter 5 before reaching the sample platform 7. The laser induced the breakdown of the film on sample platform 7 and the plasma flash occurs. Energy meter 6 reads the reflected light energy of beam splitter 5 in real-time, and computer 8 serves as the operation console. Detectors 9 and 10 are the high-speed free-space photodetectors DET08CL/M and DET25K/M produced by THORLABS. The spectral ranges that can be collected are 800–1700 nm and 150–550 nm, respectively. They are used to collect incident laser signals and thin film plasma flash signals, respectively. The optical signal of detector 9 acts as the trigger signal of detector 10. After the two optical signals are converted into electrical signals, the RT01014 four-channel oscilloscope 12 produced by Rhodes and Schwartz Company outputs and displays. The bandwidth of oscilloscope 12 is 1 GHZ and the sampling rate is 10 GHZ. Then the duration of the voltage signal of detector 10 on oscilloscope 12 is the duration of the thin film plasma flash. Due to the high energy of the incident laser, in order to protect detector 9, attenuator 11 was placed in front of it.

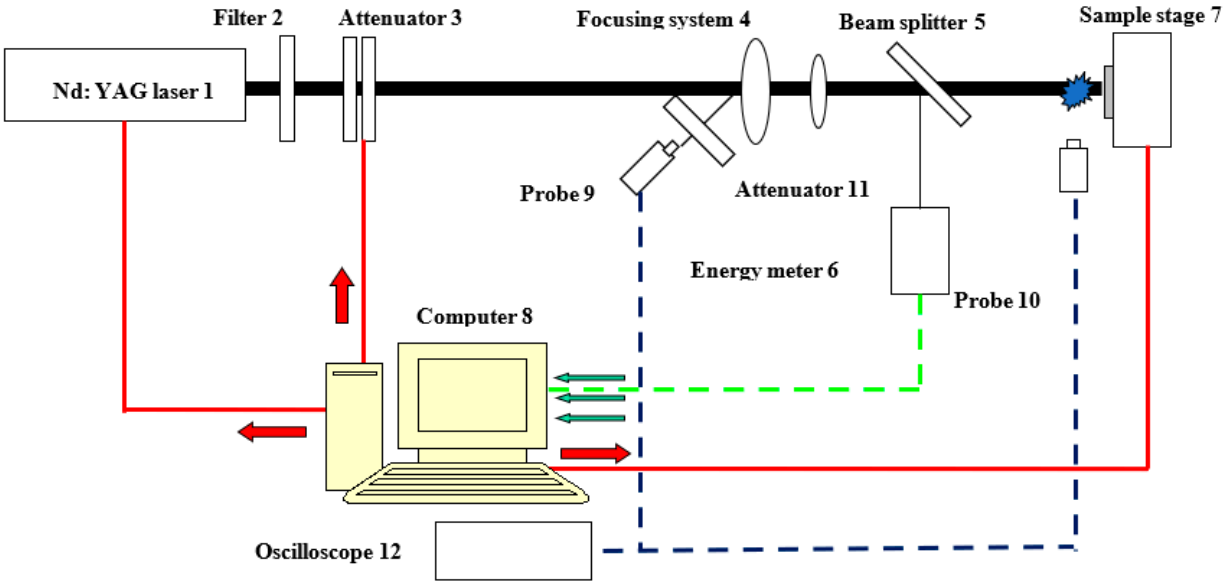

Figure 3. Schematic of the experiment.

3.2. Results and Analysis

In order to measure the duration of laser-induced thin film plasma flash, a total of 6 experiments were conducted. In experiment 1 to experiment 3, single-layer HfO_2 thin films with an optical thickness of were placed on sample platform 7, and the incident laser energies were 149.88 mJ, 122.15 mJ, and 114.66 mJ, respectively. The output signals were shown in Figures 4–6. The principle of data processing is as follows: Find a suitable voltage value U on the entire voltage signal, record its corresponding time t_1 when the signal rises to U, record its corresponding time t_2 when the signal falls to U, t_2 minus t_1 is t_f. The appropriate U selection principle is as follows: When the signal rises, the voltage between the two adjacent collection points should not differ too much, and the smaller voltage between the two collection points should be selected as U. At the same time, when the signal drops, it should be relatively slow to drop from the voltage peak of the entire signal to the corresponding voltage value U. For example, in Figure 4, when the output signal rises 100 ns, the voltage difference between two adjacent collection points is greater than 1 V. When t is 160 ns, the voltage is 1.68 V; when the next collection point t is 320 ns, the voltage rises rapidly to 2.6 V, while the signal voltage drops slowly from the peak to 1.68 V. Therefore, in the six experiments from experiment 1 to experiment 6, appropriate initial voltage values were selected for data processing for the obtained output signals. In

Figure 4, the moment when the voltage rises to 1.68 V is selected as the beginning of the thin film plasma flash, and the moment when the voltage drops to 1.68 V is selected as the end of the flash. In Figure 5, the moment when the voltage rises to 1.92 V is selected as the beginning of the thin film plasma flash, and the moment when the voltage drops to 1.92 V is selected as the end of the flash. In Figure 6, the moment when the voltage rises to 1.6 V is selected as the beginning moment of the thin film plasma flash, and the moment when the voltage drops to 1.6 V is selected as the end moment of the flash. Therefore, the duration of the thin film plasma flash t_f in Figures 4–6 can be obtained as 640.8 ns, 590.4 ns, and 574.6 ns, respectively. In experiment 4 to experiment 6, single-layer Al_2O_3 thin films with optical thickness of $\lambda/4$ were placed on sample platform 7, and the incident laser energies were 147.59 mJ, 120.87 mJ, and 112.52 mJ, respectively. The output signals are shown in Figures 7–9. In Figure 7, the moment when the voltage rises to 1.52 V is selected as the beginning of the thin film plasma flash, and the moment when the voltage drops to 1.52 V is selected as the end of the flash. In Figure 8, the moment when the voltage rises to 1.72 V is selected as the beginning of the thin film plasma flash, and the moment when the voltage drops to 1.72 V is selected as the end of the flash. In Figure 9, the moment when the voltage rises to 1.56 V is selected as the beginning moment of the thin film plasma flash, and the moment when the voltage drops to 1.56 V is selected as the end moment of the flash. Therefore, the duration of the thin film plasma flash t_f in Figures 7–9 can be obtained as 371.1 ns, 323 ns, and 314.6 ns, respectively.

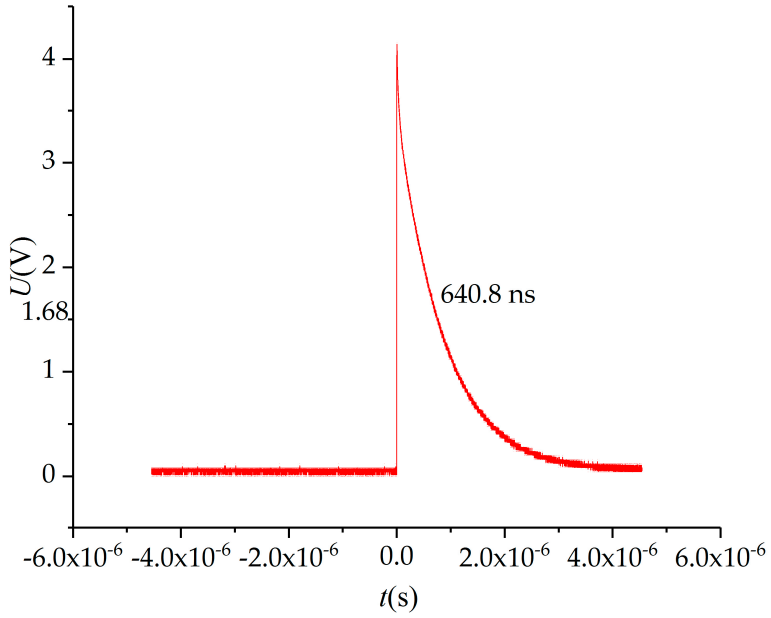

Figure 4. Signal diagram of experiment 1 (HfO_2 thin film, incident laser energy is 149.88 mJ).

The experimental value of t_f in Figures 4–9 is shown in Table 1. It can be seen from Table 1 that no matter what sample is placed in experiment 1–experiment 6, t_f increases with the increase in incident laser energy. The incident laser energy of experiment 1 and experiment 4 is similar, but the t_f obtained by them is quite different. The same conclusion is reached in experiment 2 and experiment 5, and experiment 3 and experiment 6, indicating that under the action of similar incident laser energy, the t_f of HfO_2 film is longer than that of Al_2O_3 film. This is because it is pointed out in literature [22] that, the initial velocity of HfO_2 film plasma shock wave is faster than that of Al_2O_3 film plasma shock wave, indicating that HfO_2 film plasma shock wave lasts longer, so HfO_2 film plasma flash lasts longer.

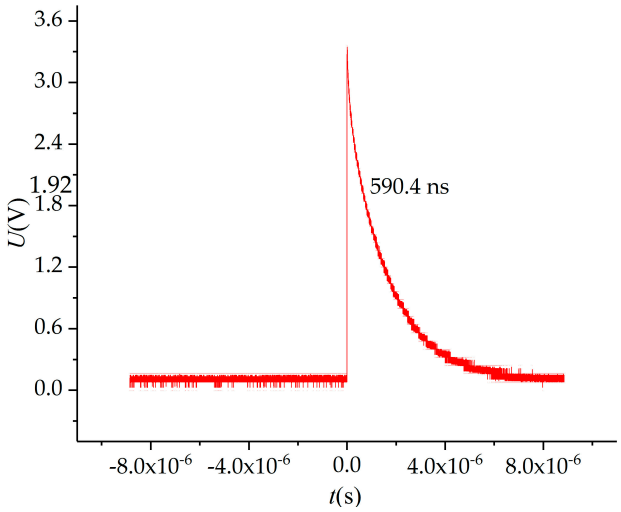

Figure 5. Signal diagram of experiment 2 (HfO_2 thin film, incident laser energy is 122.15 mJ).

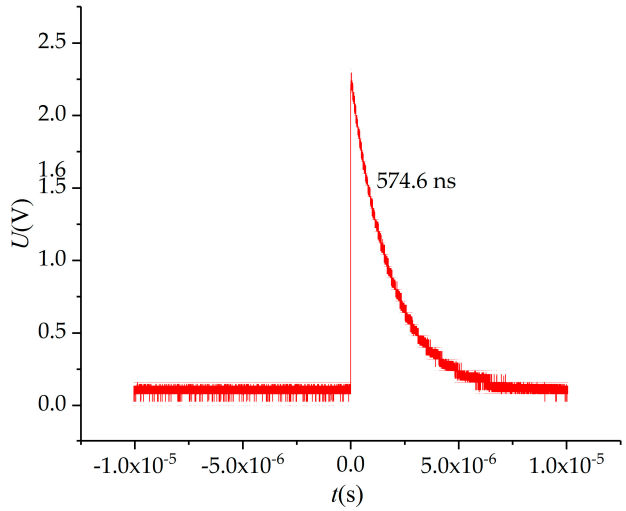

Figure 6. Signal diagram of experiment 3 (HfO_2 thin film, incident laser energy is 114.66 mJ).

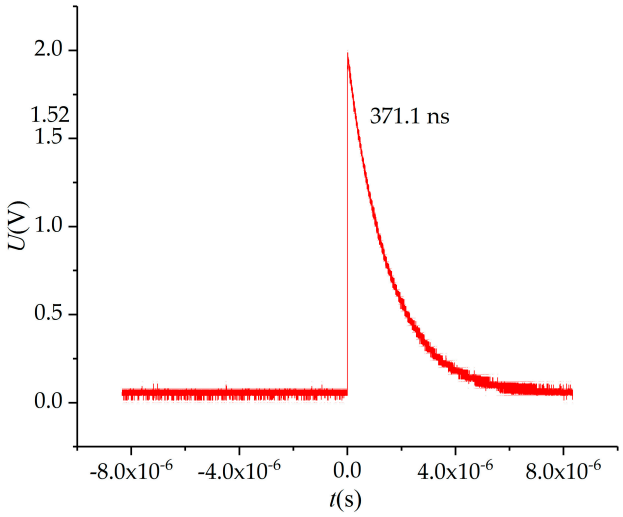

Figure 7. Signal diagram of experiment 4 (Al_2O_3 thin film, incident laser energy is 147.59 mJ).

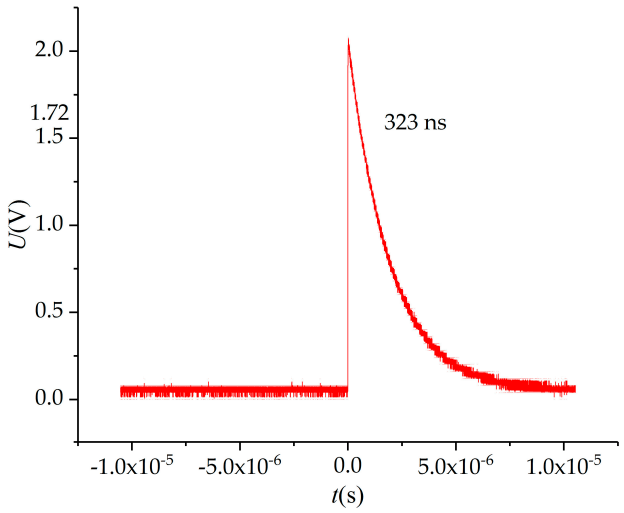

Figure 8. Signal diagram of experiment 5 (Al_2O_3 thin film, incident laser energy is 120.87 mJ).

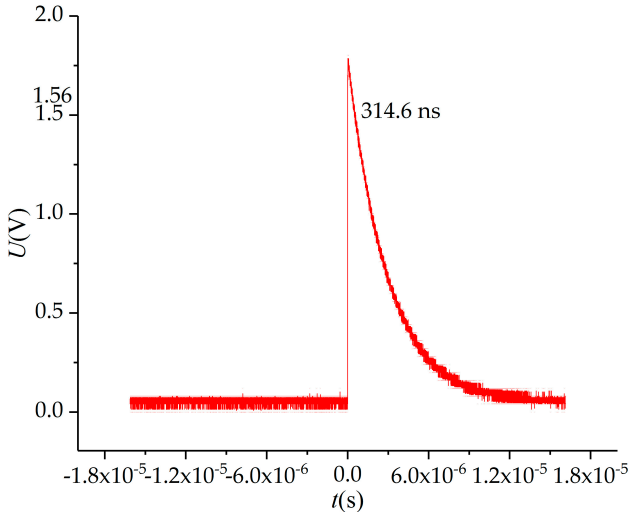

Figure 9. Signal diagram of experiment 6 (Al_2O_3 thin film, incident laser energy is 112.52 mJ).

Table 1. Experimental and theoretical values of t_f.

Experimental Number	Sample	E (mJ)	Experimental t_f (ns)	Theoretical t_f (ns)
1	HfO_2 film	149.88	640.8	640
2	HfO_2 film	122.15	590.4	588.8
3	HfO_2 film	114.66	574.6	573.8
4	Al_2O_3 film	147.59	371.1	351.1
5	Al_2O_3 film	120.87	323	323.7
6	Al_2O_3 film	112.52	314.6	314.4

Relevant parameters in the experiment are as follows: incident laser wavelength $\lambda = 1064$ nm, laser focusing spot diameter $D_s = 0.08$ cm, incident laser pulse width $t_p = 10^{-8}$ s, l of HfO_2 and Al_2O_3 film is 0.1 cm and 0.18 cm, respectively, and in these two films, $T = 10^5$ K, $N_e = 10^{19}/\text{cm}^3$. According to Formulas (2)–(6), theoretical values of t_f of the two films under different effects of E can be obtained when corresponding values of E in Table 1 are taken, respectively, as shown in Table 1.

As can be seen from Table 1, both theoretical and experimental values of t_f are in good agreement. In conclusion, both theoretical and experimental values of t_f satisfy the

following conclusions: (1) t_f increases with the increase in incident laser energy E; (2) the t_f of HfO_2 film is longer than that of Al_2O_3 film.

4. Study on Influencing Factors of the Duration of Film Plasma Flash

Due to the complexity of the ignition and sustained process of thin film plasma flash, t_f is related to many factors, such as thin film material, thin film plasma parameters, laser parameters, focusing parameters, ambient temperature, humidity, and air pressure, etc. It is assumed that the electron diffusion and adhesion during the breakdown process of thin film are ignored, and the focusing parameters, ambient temperature, ambient humidity, and air pressure, and other factors are reasonably designed. For a certain thin film, the main influences of the plasma flash duration t_f are the incident laser energy E, focused spot diameter D_s, and incident laser pulse width t_p.

The following will take Al_2O_3 thin film as an example to study the variation rule of t_f when incident laser energy E, focusing spot diameter D_s and incident laser pulse width t_p change, respectively.

4.1. Incident Laser Energy

When the incident laser energy E is changed and other parameters remain unchanged ($t_p = 10$ ns, $D_s = 0.08$ cm), the variation curve of the plasma shock wave velocity v_s of a single-layer Al_2O_3 thin film with time t can be obtained, as shown in Figure 10. As can be seen from Figure 10, with the increase in E, t_f increases, and t_f is in the order of nanoseconds.

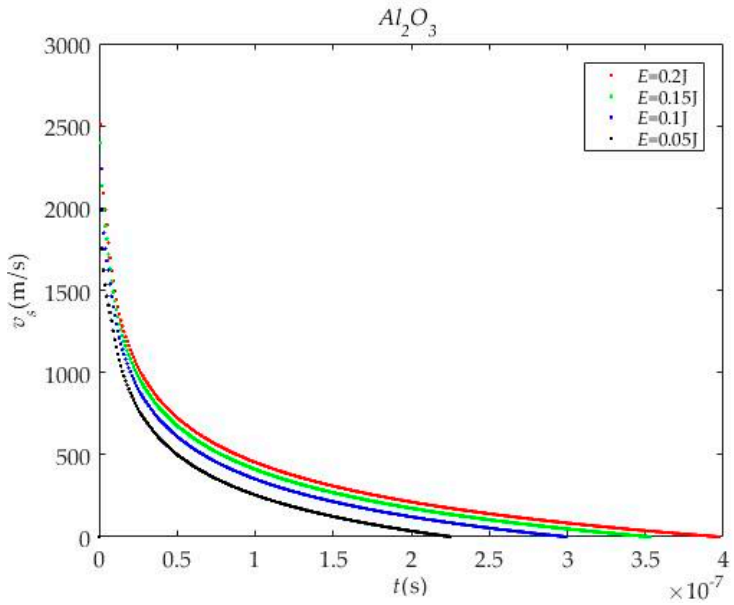

Figure 10. Curve of v_s versus t of the single Al_2O_3 film at different E.

The higher the incident laser energy, the higher the absorption laser energy of the film surface, and then the high temperature and high-density plasma is generated earlier [22]. This plasma absorbs the remaining laser energy, expands rapidly, and forms the plasma flash faster. In addition, the plasma absorbs more laser energy, so the plasma flash lasts longer.

4.2. Focusing Spot Diameter

When the focusing spot diameter D_s is changed and other parameters remain unchanged ($E = 0.1$ J, $t_p = 10$ ns), the variation curve of plasma shock wave velocity v_s of single-layer Al_2O_3 thin film with time t can be obtained, as shown in Figure 11. As can be seen from Figure 11, with the increase in D_s, t_f decreases, and t_f is in the order of nanoseconds.

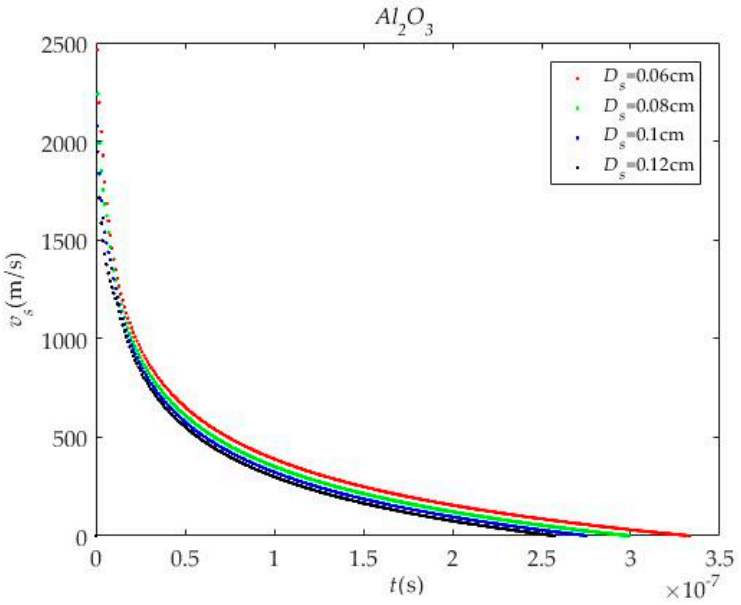

Figure 11. Curve of v_s versus t at different D_s.

As the laser energy distribution is Gaussian, the farther the film is from the focal plane of the focusing lens, the larger the laser spot area acting on the film, and the smaller the incident laser energy per unit area, resulting in slower plasma generation and less laser energy absorbed by the plasma [22], thus shortening the duration of the plasma flash.

4.3. Incident Laser Pulse Width

When the incident laser pulse width t_p is changed and other parameters remain unchanged ($E = 0.1$ J, $D_s = 0.08$ cm), the variation curve of plasma shock wave velocity v_s of single-layer Al_2O_3 thin film with time t can be obtained, as shown in Figure 12. As can be seen from Figure 12, with the increase in t_p, t_f increases, and t_f is in the order of nanoseconds.

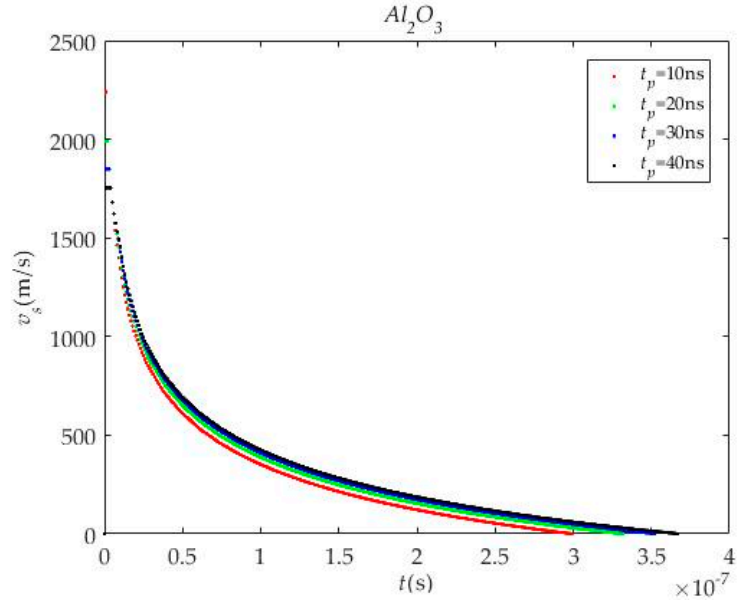

Figure 12. Curve of v_s versus t at different t_p.

Other things being equal, the larger the laser pulse width, the greater the incident laser energy absorbed by the thin film plasma, and therefore the plasma flash lasts longer.

5. Conclusions

1. The theoretical calculation model of t_f is established. When $\lambda = 1064$ nm, $D_s = 0.08$ cm, $t_p = 10^{-8}$ s, take l of HfO_2 and Al_2O_3 film are 0.1 cm and 0.18 cm, respectively [22], and take the two films $T = 10^5$ K, $N_e = 10^{19}/\text{cm}^3$, $E = 100$ mJ, the t_f of HfO_2 and Al_2O_3 film is 542.7 ns and 299.6 ns, respectively.
2. The experimental value of t_f is obtained, and the experimental parameters are put into the theoretical model to obtain the corresponding theoretical value of t_f. Through the analysis of both the experimental value and the theoretical value of t_f, it can be concluded that: ① With the increase in incident laser energy, t_f increases; ② the t_f of HfO_2 film is longer than that of Al_2O_3 film. ③ The theoretical results are in good agreement with the experimental t_f values.
3. Through calculation and analysis, it is obtained that t_f increases with the increase in E and t_p, and decreases with the increase in D_s. The process of laser induced breakdown thin film to produce plasma flash is very complicated. In this paper, only the influences of E, t_p and D_s on t_f were analyzed, respectively. In fact, t_f is also related to the film material, film plasma parameters, environmental gas type and pressure, temperature, humidity, and pre-ionization, which will be a direction of our subsequent research.
4. Because the film plasma flash duration t_f is different from the air plasma flash duration t_c, obtaining the experimental value and the theoretical value of t_f is the first step to distinguishing the two flashes. Then, as long as the air plasma flash duration t_c is obtained, the two flashes can be distinguished, thus eliminating the misjudgment caused by the plasma flash method when judging the laser film damage. The research results can improve the accuracy of damage discrimination, ensure the accurate measurement of the damage threshold of thin film laser, and have important scientific significance and practical application value for developing and enriching new damage identification methods [24,25].

Author Contributions: G.W.: validation, formal analysis, visualization, experiment, writing—original draft, writing—review and editing, data curation. J.S.: conceptualization, methodology, software, investigation, writing—review and editing, supervision, data curation. Q.W.: software, investigation. All authors have read and agreed to the published version of the manuscript.

Funding: National Natural Science Foundation of China (NSFC) (No. 61378050 and No. 62205263).

Institutional Review Board Statement: Not applicable.

Informed Consent Statement: Not applicable.

Data Availability Statement: All data that support the findings of this study are included within the article.

Conflicts of Interest: The authors declare that they have no known competing financial interest or personal relationships that could have appeared to influence the work reported in this paper.

References

1. Lai, Q.; Feng, G.; Yan, J.; Han, J.; Zhang, L.; Ding, K. Damage threshold of substrates for nanoparticles removal using a laser-induced plasma shockwave. *Appl. Surf. Sci.* **2021**, *539*, 148282. [CrossRef]
2. Zhu, C.Q.; Victor, D.; Nikolay, Y. Laser Induced Damage Threshold of Non-linear GaSe and GaSe: In Crystals upon Exposure to Pulsed Radiation at a Wavelength of 2.1 μm. *Appl. Sci.* **2021**, *11*, 1208. [CrossRef]
3. Xie, L.; Zhang, J.; Zhang, Z.; Ma, B.; Li, T.; Wang, Z.; Cheng, X. Rectangular multilayer dielectric gratings with broadband high diffraction efficiency and enhanced laser damage resistance. *Opt. Express* **2021**, *29*, 2669–2678. [CrossRef] [PubMed]
4. Lian, X.; Yao, W.D.; Liu, W.L. KNa2ZrF7: A Mixed-Metal Fluoride Exhibits Phase Matchable Second-Harmonic-Generation Effect and High Laser Induced Damage Threshold. *Inorg. Chem.* **2021**, *60*, 19–23. [CrossRef] [PubMed]
5. Shan, C.; Zhao, Y.A.; Zhang, X.H.; Hu, G.H.; Wang, Y.L.; Peng, X.C.; Li, C. Study on Laser Damage Threshold of Optical Element Surface Based on Caussian Plused Laser Spatial Resolution. *Chin. J. Lasers* **2018**, *45*, 0104002. [CrossRef]
6. Ling, X.L.; Liu, S.H.H.; Liu, X.F. Enhancement of laser-induced damage threshold of optical coatings by ion-beam etching in vacuum environment. *Optik* **2020**, *200*, 163429. [CrossRef]

7. Kumar, S.; Shankar, A.; Kishore, N.; Mukherjee, C.; Kamparath, R.; Thakur, S. Laser-induced damage threshold study on TiO_2/SiO_2 multilayer reflective coatings. *Indian J. Phys.* **2020**, *94*, 105–115. [CrossRef]
8. Xu, C.; Yi, P.; Fan, H.; Qi, J.; Yang, S.; Qiang, Y.; Liu, J.; Li, D. Preparation of high laser-induced damage threshold Ta_2O_5 films. *Appl. Surf. Sci.* **2014**, *309*, 194–199. [CrossRef]
9. Chen, L.; Lu, J.Y.; Wu, J.Y.; Feng, C.G. *Laser Supported Detonation Wave*; National Defence Industry Press: Beijing, China, 2011; p. 27.
10. Xia, Z.L.; Xue, Y.Y.; Guo, P.T.; Li, Z.; Fu, Z. The plasma burst process in laser-induced films damage. *Opt. Commun.* **2009**, *282*, 3583–3590. [CrossRef]
11. Song, Y.Z.; Liang, L. Time Distribution of the Continuum Radiation in the Plasma Induced by Laser Ablating Al. *Acta Opt. Sin.* **2001**, *21*, 404–409.
12. Cong, R.; Zhang, B.H.; Fan, J.M.; Zheng, X.F.; Liu, W.Q.; Cui, Z.F. Experimental Investigation on Time and Spatial Evolution Emission Spectra of Al Atom in Laser-induced Plasmas. *Acta Opt. Sin.* **2009**, *29*, 2594–2600. [CrossRef]
13. Nagy, T.O.; Pacher, U.; Hannes, P.; Wolfgang, K. Atomic emission stratigraphy by laser-induced plasma spectroscopy: Quantitative depth profiling of metal thin film systems. *Appl. Surf. Sci.* **2014**, *302*, 189–193. [CrossRef]
14. Lancry, M.; Poumellec, B.; Guizard, S. Comparison between Plasma Properties and Damage Thresholds in Doped Silica Exposed To IR Temtosecond Laser. *J. Laser Micro/Nanoeng.* **2012**, *7*, 217–225. [CrossRef]
15. Kim, C.K.; Lee, S.H.; In, J.H.; Lee, H.J.; Eong, S. Depth profiling analysis of $CuIn_{1-x}$ Ga_xSe_2 absorber layer by laser induced breakdown spectroscopy in atmospheric conditions. *Opt. Express* **2013**, *21*, 1018–1027. [CrossRef] [PubMed]
16. Emanuel, A.; Joerg, H.; Gabriel, S.; Laurent, M. Accurate analysis of indium–zinc oxide thin films via laser-induced breakdown spectroscopy based on plasma modeling. *J. Anal. At. Spectrom.* **2014**, *29*, 553–564.
17. Guo, L.-B.; Zhang, D.; Sun, L.-X.; Yao, S.-C.; Zhang, L.; Wang, Z.-Z.; Wang, Q.-Q.; Ding, H.-B.; Lu, Y.; Hou, Z.-Y.; et al. Development in the application of laser-induced breakdown spectroscopy in recent years: A review. *Front. Phys.* **2021**, *16*, 22500. [CrossRef]
18. Hai, R.; Tong, W.; Wu, D.; He, Z.; Sattar, H.; Li, C.; Ding, H. Quantitative analysis of titanium alloys using one-point calibration laser-induced breakdown spectroscopy. *Appl. Phys. B Laser Opt.* **2021**, *127*, 37. [CrossRef]
19. Lev, N.; Michael, G. Lasing effects in a laser-induced plasma plum. *Opt. Express* **2015**, *354*, 330–332.
20. Behera, N.; Singh, R.; Kumar, A. Confinement and re-expansion of laser induced plasma in transverse magnetic field: Dynamical behaviour and geometrical aspect of expanding plume. *Phys. Lett. A* **2015**, *379*, 2215–2220. [CrossRef]
21. Lan, H.; Wang, X.B.; Chen, H.; Zuo, D.L.; Lu, P.X. Influence of a magnetic field on laser-produced Sn plasma. *Plasma Sources Sci. Technol.* **2015**, *24*, 055012. [CrossRef]
22. Lu, J.; Ni, X.W.; He, A.Z. *Physics of Interaction between Laser and Materials*; China Machine Press: Beijing, China, 1996; p. 10.
23. Wang, G.X.; Su, J.H. Study on the mechanism of surface pressure of optical films formed by laser plasma shock wave. *Phys. Scr.* **2023**, *98*, 025607. [CrossRef]
24. John, A. Thornton. Plasma-assisted Deposition Processes: Theory, Mechanisms and Applications. *Thin Solid Film.* **1983**, *107*, 3.
25. Ujjwal; Kumar, R. Optical Frequency Comb Generator Employing Two Cascaded Frequency Modulators and Mach–Zehnder Modulator. *Electronics* **2023**, *12*, 2762. [CrossRef]